Published in final edited form as:
Phys Med Biol. 2012 June 7; 57(11): R99–R117. doi:10.1088/0031-9155/57/11/R99.

Range uncertainties in proton therapy and the role of Monte Carlo simulations

Harald Paganetti
Department of Radiation Oncology, Massachusetts General Hospital and Harvard Medical School, Boston, MA 02114

Abstract

The main advantages of proton therapy are the reduced total energy deposited in the patient as compared to photon techniques and the finite range of the proton beam. The latter adds an additional degree of freedom to treatment planning. The range in tissue is associated with considerable uncertainties caused by imaging, patient setup, beam delivery and dose calculation. Reducing the uncertainties would allow a reduction of the treatment volume and thus allow a better utilization of the advantages of protons. This article summarizes the role of Monte Carlo simulations when aiming at a reduction of range uncertainties in proton therapy. Differences in dose calculation when comparing Monte Carlo with analytical algorithms are analyzed as well as range uncertainties due to material constants and CT conversion. Range uncertainties due to biological effects and the role of Monte Carlo for in vivo range verification are discussed. Furthermore, the current range uncertainty recipes used at several proton therapy facilities are revisited. We conclude that a significant impact of Monte Carlo dose calculation can be expected in complex geometries where local range uncertainties due to multiple Coulomb scattering will reduce the accuracy of analytical algorithms. In these cases Monte Carlo techniques might reduce the range uncertainty by several mm.

1. Introduction

The number of patients being treated with proton therapy is steadily increasing in radiation oncology. The main reason for the increased interest in proton therapy is the physical characteristics of the depth dose curve with a dose peak (Bragg peak) at a well-defined depth in tissue, which was first recognized as potentially useful for cancer therapy by Wilson (Wilson, 1946). The total energy deposited in a patient (often termed ‘integral dose’) for a given target dose is always lower when using proton as compared to photon treatment techniques. This is in part due to the lack of exit dose. Furthermore, the Bragg peak allows, in theory, to point a beam directly towards a critical structure, increasing the flexibility of proton therapy treatment planning compared to conventional photon therapy. A short overview of proton therapy delivery techniques is given elsewhere (Paganetti and Kooy, 2010).

In order to fully utilize the potential advantage when using protons, the range of proton beams in patients needs to be predicted as accurate as possible in the treatment planning and delivery process. An improper quantification of safety margins can have more sever consequences in proton therapy than in photon therapy. Margins underestimating uncertainties in photon therapy might cause under-dosage of the tumor. In proton therapy, such an underestimation may cause part of the tumor not receiving any dose due to a potential shift of the sharp distal dose fall-off.

Uncertainties in the exact position of the distal dose gradient arise from a) organ motion, b) setup and anatomical variations, c) dose calculation approximations, and d) biological considerations. At the Massachusetts General Hospital (MGH), treatment planning assumes an uncertainty in the proton beam range of 3.5% of the range plus an additional 1mm. Other centers follow similar margin recipes. For example, the MD Anderson Proton Therapy Center in Houston, the Loma Linda University Medical Center, and the Roberts Proton Therapy Center at the University of Pennsylvania all apply 3.5% + 3mm while the University of Florida Proton Therapy Institute uses 2.5% + 1.5mm1. The 3.5% + 1mm range margin at MGH, for instance, results in a deliberate overshoot of 8mm for a 20 cm range field in soft tissue, which is quite substantial. Note that these margins are often not fully generic and that adjustment may be made for certain sites based on the location of critical structures.

Monte Carlo techniques are being used in proton therapy for years. However, the improved accuracy of Monte Carlo as compared to analytical dose calculation techniques had no influence on the margin recipes so far. Comparisons of the two dose calculation techniques reveal in general differences that are clinically insignificant because conservative treatment margins minimize the impact of dose calculation (e.g. range) uncertainties. Progress in radiation therapy and decrease in normal tissue complication probability can be achieved in part through the reduction of treatment volumes. Only if we understand range uncertainties will we feel comfortable to reduce the range margin. As part of an international workshop on “Recent Advances in Monte Carlo Techniques for Radiation Therapy” we tried to answer the question whether Monte Carlo dose calculation might be able to contribute to this quest. This article summarizes the presentation given at this meeting. It does focus on static cases without organ motion.

2. Range definition

Due to range straggling, not all protons of the same energy have the same range. Thus, the range needs to be defined for a beam of protons resulting in a broadened Bragg peak or a spread-out Bragg peak (SOBP). Ideally the range would be defined at the position where the dose has decreased to 80% of the maximum dose, i.e. in the distal dose falloff. The reason for this choice is the fact that for a monoenergetic proton beam, the 80% fall-off position coincides with the mean projected range of a proton, i.e. the range at which 50% of the protons have stopped. Furthermore, the 80% fall-off position is thus independent of the beam’s energy spread. Nevertheless, in most proton therapy facilities, the prescribed range is defined at the 90% fall-off position in water or the 90% isodose line in a patient because of historic reasons. Figure 1 shows the energy-range relationship for monoenergetic proton beams.

3. Studies on range uncertainties in proton therapy

3.1 Range uncertainties due to multiple Coulomb scattering

While Monte Carlo based treatment planning systems are slowly entering the market, most current commercial planning systems are based on analytical pencil-beam dose calculation algorithms. Differences between Monte Carlo based dose calculation and analytical methods in proton therapy have been demonstrated (Paganetti *et al.*, 2008; Petti, 1996; Schaffner *et al.*, 1999; Soukup and Alber, 2007; Soukup *et al.*, 2005; Szymanowski and Oelfke, 2002; Tourovsky *et al.*, 2005; Titt *et al.*, 2008a). In addition, experimental validations have been

[1]Personal communications by Stephen Avery (Roberts Proton Therapy Center at the University of Pennsylvania), Zuofeng Li (University of Florida Proton Therapy Institute), Radhe Mohan (MD Anderson Proton Therapy Center, Houston), and Baldev Patyal (Loma Linda University Medical Center).

done in simple geometries. If we consider Monte Carlo to be the gold standard (although there are physics uncertainties in the Monte Carlo as well; see below) we can assess the range uncertainty due to dose calculation in complex geometries by comparing the range predicted by the treatment planning system with the range predicted by a Monte Carlo simulation.

Analytical dose calculation algorithms typically project the range based on the water equivalent depth in the patient neglecting the position of inhomogeneities relative to the Bragg peak depth (Petti, 1992, 1996; Urie *et al.*, 1984). Furthermore, such algorithms are less sensitive to complex geometries and density variations, e.g. at bone-soft tissue interfaces. Consequently, analytical algorithms are not able to correctly predict the effect of range degradation caused by multiple Coulomb scattering (Sawakuchi *et al.*, 2008; Urie *et al.*, 1986; Goitein, 1977; Goitein and Sisterson, 1978). Figure 2 illustrates the effect in a regular geometrical grid with alternating high and low density material based on a Monte Carlo study (Sawakuchi *et al.*, 2008). The authors analyzed range degradation effects as a function of proton energy and geometric complexity. It was found that the difference in the 80% to 20% falloff position is in the order of ~2mm for a 220 MeV beam. At the 90% falloff the figure shows a difference in range of about 1.5mm, i.e. −0.7%.

While in such a regular structure range degradation causes mainly a simple widening of the distal fall-off, the effects in a complex patient geometry are not as easy to predict. For an SOBP penetrating a human skull, it was reported that dose degradation in the distal falloff can reduce the range at the 80% dose level by up to 8mm, depending on the density variation (Urie *et al.*, 1986). This worst case did affect only a small region of the distal dose distribution. Another example is shown in figure 3. Here, multiple Coulomb scattering at a bone-soft tissue interface tangential to the beam, in the penumbra, causes a scatter dis-equilibrium. The result is a range variation affecting a small part of the distal fall-off only. This effect can be understood considering the simple geometry in figure 4. Range perturbations due to multiple Coulomb scattering in complex structures cannot be modeled using solely the stopping power of materials involved and their water equivalent path length, which would simply cause a shift in the distal falloff.

While for large fields these might be local effects, for very small fields in the head and neck region these effects can potentially affect the majority of the treatment volume as seen in figure 5 (Bednarz *et al.*, 2010). The figure illustrates a dose non-uniformity in the target predicted by Monte Carlo but not by the treatment planning system. The effect of range degradation as illustrated by the step in the distal part of the depth dose distribution is quite substantial on the 95% dose level but almost negligible at the 90% level. The example is for a small field with complete lack of lateral equilibrium and thus not a typical scenario. For these, the range effects seen in figures 3 and 5 can be estimated to be on the order of ±2.5%. Note that the dose discrepancy near the entrance region is due to scattering from the aperture located close to the patient, which is not considered by the analytical algorithm. The impact of edge-scattered protons has been studied previously (Titt *et al.*, 2008b; van Luijk *et al.*, 2001). Not modeled accurately in analytical dose calculations will affect mainly the proximal part of the Bragg curve, except for very shallow fields.

3.2 Monte Carlo uncertainties due to physics

In the previous section we have shown that analytical dose calculations do have limitations when it comes to predicting the correct proton beam range. However, there are also uncertainties when using Monte Carlo methods. Three codes used in proton therapy (Geant4 (Agostinelli *et al.*, 2003), FLUKA (Ferrari *et al.*, 2005), and MCNPX (Pelowitz, 2005)) were compared with each other and with measurements by Kimstrand et al (Kimstrand *et al.*, 2008). The physics settings within the codes were varied when simulating small angle

scattering at aperture edges where small uncertainties in scattering power would be detectable. A significant impact of user-defined parameters was found. One has to keep in mind that most Monte Carlo codes used in proton therapy were originally developed for high-energy physics applications and span a wide range of particles and energy domains. There can be uncertainties due to the implementation of physics interactions via theoretical models or interpolation of experimental data. The accuracy of physics settings might depend on the energy region of interest. Thus, the default physics models might not be tailored for proton therapy simulations and may require adjustment (Herault *et al.*, 2005; Stankovskiy *et al.*, 2009; Pia *et al.*,2010; Zacharatou Jarlskog and Paganetti, 2008). It is the responsibility of Monte Carlo users to benchmark their code and understand the impact of incorrect physics settings. In particular, uncertainties in nuclear interaction probabilities can be substantial because most experiments were done decades ago on thin targets resulting in data for one specific energy only. Thus, most cross sections are known over the entire energy region of interest. Fortunately, nuclear cross section uncertainties are largely inconsequential for the predicated range from dose calculations because of the low proton energies (below the nuclear interaction threshold) at the distal falloff of a Bragg curve.

A validation of Monte Carlo dose calculation methods is typically done using homogeneous or heterogeneous geometries consisting of various materials (Paganetti *et al.*, 2004; Paganetti *et al.*,2008; Titt *et al.*, 2008a). Beam profiles in water downstream of inhomogenous targets and compensators have been used to analyse the multiple scattering theory can vary from Moliére's theory (Andreo *et al.*, 1993; Gottschalk *et al.*,1993). For instance, the code Geant4 uses a condensed history algorithm for multiple scattering that utilizes functions to calculate the angular and spatial distributions of the scattered particle implementations (Urban, 2002).

While discrepancies between different multiple Coulomb scattering implementations might be negligible, the uncertainties in the mean excitation energy are presumably significant. The two main parameters in the Bethe-Bloch equation that determine the range are the density and the mean excitation energy. In its report from 1993, the ICRU (ICRU, 1993) recommends a mean excitation energy, or I-value, of 75±3 eV for water. Others have reported 80±2 eV (Bichsel and Hiraoka, 1992). The stopping power tables by Janni (Janni, 1982) are based on a value of 81.8 eV while a more recent experimental study resulted in a value of 78.4±1.0 eV (Kumazaki *et al.*, 2007). Andreo (Andreo, 2009) has demonstrated that a variation of I-values between 67.2 eV and 80 eV can have a substantial impact on the proton beam range in water (see figure 6). It was concluded that the range uncertainty due to uncertainties in I-values is on the order of ±1.5–2.0%. However, the lower boundary can most certainly be excluded based on recent measurements. The difference in I-value between 75 and 80 eV results in a 0.8–1.2% difference in the predicted stopping power in the therapeutic energy range.

Even if the Monte Carlo predicted range is normalized to the expected range based on measurements in water, there are still uncertainties in tissues based on their material compositions. Mean excitation energies for various elements are tabulated by the ICRU (ICRU, 1993), which also includes averaged values for tissues (ICRU, 1989, 1992). Mean excitation energies are typically adjusted to agree with measurement or interpolated where such data are not available. Theoretical models have uncertainties, for example due to binding effects (Ahlen, 1980). For tissues, the uncertainty in I-value is potentially on the order of 10–15% (Andreo, 2009). This might result in a range uncertainty in tissue of ~1.5%.

For complex passive scattered delivery systems, Monte Carlo dose calculation is often based on a complete simulation of the treatment head geometry. A SOBP is created by varying the

beam energy by using a rotating absorber consisting of several steps of water-equivalent thicknesses. The beam current is typically modulated as a function of the wheel rotational angle. A double-scattering system creates a broad beam. Patient specific apertures and compensators ensure lateral and distal target conformation. Figure 7 shows a simulated proton therapy treatment head. There are several uncertainties in addition to I-values in treatment head modeling that can cause Bragg curves to differ slightly from measured ones. The vendor's blueprints may deviate slightly from the built devices. Furthermore, uncertainties are introduced because material compositions might not be known with sufficient accuracy. For example, Carbon used in scattering devices can be purchases in various different densities.

A comprehensive study on the uncertainties in treatment head modeling was done by Bednarz et al. (Bednarz *et al.*, 2011). Specifically the sensitivity of SOBP dose distributions on material densities, mean excitation energies, initial proton beam energy spread and spot size was investigated. Densities were varied by up to ±5% and I-values were varied by up to ±20%. For a treatment head simulation based on the MGH gantry (Paganetti *et al.*, 2004) there was a 4% range uncertainty due to uncertainties in densities of lead and lexan. Furthermore, the mean excitation energies caused an uncertainty of up to 2%. Note that the parameter variations may be too generous depending on the quality of the vendor information.

Some of the uncertainties in treatment head modeling cannot be overcome because exact geometrical or material information from the vendor might not be available. On the other hand adjusting parameters to match a specific range and modulation width can have a negative impact on other range/modulation width combinations. An alternative method to fine-tune a treatment head model is to optimize the time-dependent beam current modulation functions to improve the agreement between calculated and measured SOBP dose distribution to within clinical tolerance levels (Bednarz *et al.*, 2011).

3.3 Monte Carlo uncertainties due to CT conversion

In proton therapy planning systems, Hounsfield unit (HU) conversion schemes are implemented to translate HU into relative stopping power. Conversion schemes are typically based on CT scans of tissue phantom materials with known density and elemental composition. The relationship between stochastic errors, i.e. noise, in CT images and the predicted proton beam range has been studied by Chvetsov and Paige (Chvetsov and Paige, 2010). They reported a standard deviation of the range between ~0.3% and ~0.7% assuming a CT grid of 3mm and a 2.5% noise level. An error below 1% on the stopping power values was reported based on dual energy CT (Yang *et al.*, 2010).

Even small discrepancies in the calculated local energy deposition can result in significant changes in range because they may accumulate over the entire beam path (Jiang and Paganetti, 2004; Matsufuji *et al.*, 1998; Mustafa and Jackson, 1983). A range uncertainty margin of 0.82% was suggested by Matsufuji et al. (Matsufuji *et al.*, 1998). Density variations alone might cause an uncertainty below 1% because of the small spread of densities for tissues corresponding to the same HU. The range uncertainty of the conversion method based on a stoichiometric conversion using animal tissues has been reported to be up to 1.8% for bone and 1.1% for soft tissues translating into a range uncertainty of 1–3mm (Schaffner and Pedroni, 1998). These numbers do include the uncertainty in the I-value. Thus, the pure uncertainty due to stopping power conversion is presumably ~0.5%.

For Monte Carlo simulations, not relative stopping power but density and material composition are assigned. Various approaches of material/density conversions have been published (du Plessis *et al.*, 1998; Schneider *et al.*, 1996; Schneider *et al.*, 2000;

Vanderstraeten *et al.*, 2006). The stopping power is only slightly affected by uncertainties in the carbon, oxygen and nitrogen weight fractions because they have very similar atomic number to atomic mass ratio. It is more sensitive to hydrogen weight fraction. On the other hand, the uncertainty of hydrogen weight fraction obtained from a stoichiometric calibration is negligible for most tissues (Schneider *et al.*, 2000). Consequently, CT conversion uncertainties using Monte Carlo should be smaller than the ones for analytical dose calculation. It has been shown that if the HU conversion is based on a proper stoichiometric calibration, the uncertainties on the proton beam range for head and neck patients is likely below 0.5mm (~0.2%) (Espana and Paganetti, 2010).

While each HU is assigned a unique density, the number of material composition assignments is typically much smaller. Fewer tissue (i.e. material compositions) do increase the efficiency of Monte Carlo simulations as physics settings are typically generated for each tissue separately on the fly. It was shown that the number of different tissues defined in a Monte Carlo simulation should be larger than ~10 to avoid an impact on the proton beam range (Espana and Paganetti, 2010).

Note that when using a conversion scheme for clinical dose calculation it has to be normalized to the departmental CT scanner. This can be done, for example, by simulating a HU versus relative stopping power conversion curve in the Monte Carlo setting and then normalize this to the clinical conversion curve by slightly adjusting the HU versus density relationship in the Monte Carlo (Jiang and Paganetti, 2004).

Potential CT artifacts can also affect the accuracy of proton range prediction based on CT images. These are particularly severe in the presence of metallic implants (Jaekel and Reiss, 2007; Newhauser *et al.*, 2008). We have not included this specific scenario in our range uncertainty analysis.

Finally, Monte Carlo simulations typically report dose-to-tissue as compared to dose-to-water reported by a planning system based on an analytical dose calculation method. In order to compare the two systems one needs to convert the dose. Such a conversion can be done based on relative stopping powers and additional terms considering nuclear interactions (Paganetti, 2009). Reporting dose-to-tissue can result in a slightly different range compared to reporting dose-to-water, specifically in bone (Paganetti, 2009). The discrepancy can be on the order of 1–2mm in an extreme case. We do not consider this an additional uncertainty because clinical decisions are solely made based on dose-to-water.

3.4 Monte Carlo uncertainties due to CT resolution

In a relatively homogeneous geometry the size of the voxels used to divide the geometry for dose calculation plays a minor role. Even for typical head and neck cases significant uncertainties might not be expected based on the CT resolution typically used for treatment planning. Problems could be encountered in highly heterogeneous geometries where the heterogeneities are small, like in lung. Here, materials with low density, i.e. air, and materials with considerably higher density, i.e. soft tissue, might be averaged to obtain the HU for a given voxel. To study this effect a swine lung was CT scanned with fine resolution of $0.4\times0.4\times0.2$ mm^3 (Espana and Paganetti, 2011). Monte Carlo simulations were used to compare the dose distributions predicted with the voxel size typically used in treatment planning with those expected to be delivered using a finer resolution. CT images with $0.8\times0.8\times1.2$ mm^3 as well as $0.8\times0.8\times2.4$ mm^3 voxel size were created from the fine resolution scan by combining and interpolating HU. Figure 8 shows the CT scan of the swine lung. An artificial rectangular tumor was simulated to study range variations in a homogenous field with a horizontal dose-fall off downstream of the sharp edge of the artificial tumor.

The range when defined as the mean distal falloff position at 90% of the maximum dose varied by 2.4mm between the fine and the course resolution (used for planning). At the 50% falloff position the differences were up to 5.6mm. The maximum difference was 38 mm when airways were present in the beam path. Depending on the region of the lung, the standard deviation was up to 1cm. The differences are due to the poor axial resolution of CT images typically used in clinical routine. The lung case can be seen as a worst-case scenario. The maximum differences hold for one ray, which would be smoothed out due to intrafractional motion and interfractional variations. For sites outside of the lung, the range uncertainty due to CT resolution might be estimated to only about 0.3% for CT resolutions typically used in treatment planning.

3.5 Range uncertainties due to biological effects

Proton therapy uses a generic value for the relative biological effectiveness (RBE) to relate prescribed proton doses to photon doses (Paganetti *et al.*, 2002). The RBE is a function of dose, tissue endpoint and energy deposition characteristics. The latter is important with respect to range uncertainties. For a given dose and biological endpoint in proton therapy one can parameterize the energy deposition characteristics by the linear energy transfer (LET). The increasing LET with depth in an SOBP is compensated by a decreasing proton fluence resulting in a homogeneous depth-dose distribution. The increase in LET causes an increase in the RBE at the distal end of the SOBP. This in turn causes a shift in the biologically effective range by ~1–2mm due to an LET increase and a dose decrease (Paganetti and Goitein, 2000; Robertson *et al.*, 1975; Wouters *et al.*, 1996). The effect is illustrated in figure 9. Unfortunately, even if we can predict LET distributions to a reasonable accuracy using Monte Carlo simulations (Grassberger and Paganetti, 2011), the knowledge of biological parameters on dose and endpoint dependency is not sufficient to perform biological, RBE based, treatment planning with sufficient accuracy.

A potential approximation is the use of voxel-by-voxel LET information for biologically optimized treatment planning, i.e. use elevated LET values as constraints in treatment planning so that they can be steered away from critical structures as much as possible (Grassberger *et al.*, 2011). Figure 10 shows two treatment plans and the respective dose-averaged LET distributions illustrating the concept. This method does not directly address biological range uncertainties but minimizes their impact for a given treatment plan in intensity-modulated proton therapy.

The shift of the distal fall-off due to an RBE in excess of 1.1 has been seen for tissues with low α/β ratio. For tissues with high α/β ratio the RBE at the distal falloff might not exceed 1.1 (it might even be below 1.1 in the center of the SOBP) causing no significant range shift. Thus, the RBE effect should not be included in the clinical range uncertainty margin because it will presumably always result in a potential range increase. In contrast, the biological uncertainty (~0.8%) should be included in a margin increase for organs at risk if beams are pointing towards them.

3.6 In vivo range verification

Uncertainties could be better understood if in vivo range verification could be done with high precision. The most frequently used method uses positron emission tomography (PET) imaging, i.e. imaging of the activation of the patient's tissue by the proton beam (Parodi and Enghardt, 2000; Parodi *et al.*, 2007; Knopf *et al.*, 2009; Knopf *et al.*, 2011). Proton nuclear interactions in the patient create positron emitters such as ^{11}C ($T_{1/2}$=20.39 min), ^{13}N ($T_{1/2}$=9.97 min), and ^{15}O ($T_{1/2}$=2.04 min). A similar method in terms of the underlying physics is the detection of prompt gamma radiation emitted after nuclear excitation by the proton beam in tissue (Polf *et al.*, 2009a; Polf *et al.*, 2009b). Interestingly, for the latter

method, the maximum in the cross section as a function of energy is at lower energies compared to the PET isotope production cross sections. This causes the prompt gamma signal maximum to be closer to the Bragg peak than the PET signal maximum (Moteabbed *et al.*, 2011). Another advantage compared to the PET method is a potentially higher count rate. However, currently detector efficiencies are not able to utilize this advantage leaving PET as the only practical method at this time. Finally, it has been shown that magnetic resonance imaging (MRI) done weeks or months after treatment can reveal range information due to tissue changes, e.g. fatty replacements at the spinal cord (Gensheimer *et al.*, 2010). Detectors placed inside the human body have also been suggested (Lu, 2008a, b).

PET range verification has been done at several institutions. Relevant for this article is the capability of Monte Carlo methods to predict the correct PET isotope production. Proton beams loose energy mainly via electromagnetic interactions. Consequently, the activation image from PET imaging is not directly correlated to the dose distribution. The established method is to use a Monte Carlo calculated distribution of the positron emitters and compare this predicted image with a measured image. The accuracy depends on the underlying cross section data (Litzenberg *et al.*, 1999; Oelfke *et al.*, 1996; Parodi *et al.*, 2005). The implementation of inelastic nuclear interactions into a Monte Carlo system can be complex. One has to rely on a model (or a combination of models) with empirical parameter sets or experimental cross section data associated with considerable uncertainties. The reason for the uncertainties in cross sections is based on the fact that the relevant physics experiments (mostly done in the 50's, 60's and 70's) have focused on thin targets thus determining cross sections for a distinct energy. However, in proton therapy we are interested in a thick target stopping the entire beam and thus in a continuous cross section information over the entire energy region of interest.

To study the uncertainty in the predicted range deduced from PET imaging due to uncertainties in measured cross section data used in the Monte Carlo simulation, a study was done using a heterogeneous phantom consisting of various materials (Espana *et al.*, 2011). Studied were the reactions $^{16}O(p,pn)^{15}O$, $^{12}C(p,pn)^{11}C$ and $^{16}O(p,3p3n)^{11}C$. Several published experimental and theoretical cross section data were implemented in a Monte Carlo system. The predicted PET images were then compared with measured PET images. The different cross section data resulted in range differences below 1 mm when a 5 min scan time after treatment was employed but up to 5 mm for a 30 min scan time with 15 min additional delay (a typical scenario for off-line out-of-the room PET range verification). Figure 11 shows one example using a gel with high oxygen concentration and two different experimental cross section data sets from the EXFOR database (EXFOR/CSISRS, 2010), the cross section published by the ICRU (ICRU, 2000) and a combination of the ICRU cross section recommendation with the experimental data that was obtained by using an envelope encompassing the available data points (Espana *et al.*, 2011). The conclusion of this study was that more experimental data in particular for the $^{16}O(p,3p3n)^{11}C$ reaction channel are needed to reduce the uncertainties in Monte Carlo simulations to below 1 mm. Note that in addition to uncertainties in cross sections when comparing measured PET images with Monte Carlo simulations, there are other inherent limitations of PET range verification, e.g. scanner resolution, biological washout etc. (Knopf *et al.*, 2009).

4. Discussion

In proton therapy treatment planning the prescribed range is increased to account for uncertainties in the predicted proton beam range. The guidelines depend on the proton therapy facility and generally include a generic margin recipe that might however be revised for specific treatment scenarios. The recipe at Massachusetts General Hospital, 3.5% of the prescribed range + 1mm, was originally introduced at the Harvard Cyclotron Laboratory

based on estimations published in a paper by Goitein (Goitein, 1985) and was supposed to include two factors2. The first one was an absolute value of about 1 mm based on the uncertainty in patient setup, detection of the skin surface and compensator design. The second factor was based on the uncertainty associated to CT imaging and conversion. With the CT technology and resolution of the early 1980's, the uncertainty in determining HU values was estimated as 2%. Another 1% was added for the CT conversion uncertainty leading to water equivalent densities in tissue. This lead to $\sqrt{(2\%^2+1\%^2)}\times 1.5$ standard deviations or ~3.5%. Thus, interestingly, the definition of this original range uncertainty recipe did not include uncertainties due to dose calculation, other than those associated with the water equivalent density. On the other hand, CT scanners have improved quite a lot since the early 1980's. Based on the findings summarized above we can try to estimate the current range uncertainties in proton therapy and the potential impact of Monte Carlo.

First there are those uncertainties that are independent of dose calculation. These are mainly uncertainties in commissioning, compensator design, beam reproducibility and patient setup. They have been estimated in table 1. Note that the patient setup error is the range uncertainty due to a setup uncertainty of ~1mm, not the setup uncertainty itself.

The uncertainties due to dose calculation are caused by defining the patient geometry using CT and by the dose calculation algorithm itself. The uncertainty from CT imaging itself and scanner calibration might be ±0.5% for today's technology (see 3.3). Another contribution is caused by the conversion of HU into relative stopping power or material composition (leading to stopping power). Based on the discussion above one might assume ±0.5% for analytical calculations and ±0.2% for Monte Carlo simulations (see 3.3). The CT grid certainly plays a role but this effect is presumably only significant (bigger than a few %) in lung and, potentially, in bone or at interfaces of bone and soft tissue. We might assume a ±0.3% effect for a site with typical density variations (see 3.4).

If we assume that pristine peaks in water have been normalized to measured data both for the Monte Carlo and the analytical planning system, the residual range difference between Monte Carlo and analytical dose calculation method is mainly caused by a) uncertainties in stopping power in tissue (i.e. mostly due to the I-value) and b) multiple Coulomb scattering causing range degradation. The latter can be divided into two effects. First, homogeneities lateral to the beam path causing scatter disequilibrium (see 3.1) are not modeled correctly in a typical analytical model, which can lead to significant differences between the two dose calculation methods, i.e. ±2.5% (see figures 3 and 5). This effect would however affect only a small volume within the treatment field and should not be considered as a range uncertainty in all treatment scenarios as it would only appear for certain geometries and beam arrangements. Thus, it might not be included in a generic margin recipe. Second, the depth of inhomogeneities not considered in a typical analytical model based on water equivalent pathlengths. This effect might be smaller causing an uncertainty on the order of 0.7% (see 3.1). In contrast, the physics uncertainties in a Monte Carlo model are presumably below ±0.1%.

The uncertainties in stopping power are mainly due to the I-value but also du to the HU conversion method. Note that the uncertainty in stopping power ratio discussed above (1.1–1.8% (Schaffner and Pedroni, 1998)) includes both. One may assume a range uncertainty in water of ~1.2% (see 3.2) caused by the I-value alone and thus an uncertainty in tissue of maybe ±1.5%, which affects all dose calculation methods equally.

[2]M. Goitein, personal communication

Furthermore, there are uncertainties due to biological considerations (see 3.5). Uncertainties due to variations in RBE at the distal falloff depend on the biological endpoint (e.g. the α/β ratio of the tissue). On average, the uncertainty might be ~0.8%. An exception could be tissues with very small α/β ratios where this uncertainty might be bigger. In the calculation of the added range uncertainty, biological effects were excluded because they would only increase the range.

Table 1 lists the main sources of uncertainty for nonmoving targets. Most uncertainties do depend on the beam energy or range so that it is appropriate to give uncertainties in % rather than mm. The estimations are for soft tissues and bone. As discussed above, lung might show a much bigger impact on CT imaging uncertainties, possibly up to 5%, and uncertainties due to the large water-equivalent range in low-density lung tissue. Also not included are effects from CT artifacts and organ motion. Note also that not all sources in table 1 are truly independent. For instance, a setup error impacting the beam path could influence range degradation effects significantly. The appropriate range uncertainty margin might depend on the ability to avoid dosimetrically challenging beam directions.

The total estimated uncertainties are displayed in figure 12. It seems that the current practice at most centers might be too conservative. A range uncertainty of 2.7%+1.2mm was deduced based on the estimations given above. It appears that introducing routine Monte Carlo dose calculation would not have much of an impact for a typical case as long as the main source of uncertainty is remains, i.e. the uncertainties in the mean excitation energies. A highly significant impact of Monte Carlo dose calculation can be expected though in complex geometries where local range uncertainties due to multiple Coulomb scattering will reduce the accuracy of pencil beam algorithms significantly. The magnitude of the discrepancy might of course also depend on the quality of the analytical algorithm. It might well be possible to design an analytical algorithm that comes close to the Monte Carlo results.

The impact of differences in the predicted range between Monte Carlo dose calculation and analytical dose calculation and the resulting range that has to be prescribed in treatment planning to account for dose calculation uncertainties, depends on the treatment site. It seems advisable that range uncertainties included in treatment planning should not be based on generic recipes but depend on patient geometry and treatment planning considerations. Potentially, a method based on a heterogeneity index (Pflugfelder *et al.*, 2007), which parameterizes the heterogeneous geometry along the beam path, could be applied to define the most appropriate distal (range) margin due to expected dose calculation errors for a given site and beam direction or identify those cases where Monte Carlo dose calculation is desired. Obviously, the uncertainty also depends on the specific geometry in the beam path and the treatment plan, i.e. the beam angles. Robust optimization techniques can be applied to minimize range uncertainties (Unkelbach *et al.*, 2007).

Acknowledgments

This work was funded in part by NIH/NCI PO1 CA21239.

References

Agostinelli S, Allison J, Amako K, Apostolakis J, Araujo H, Arce P, Asai M, Axen D, Banerjee S, Barrand G, Behner F, Bellagamba L, Boudreau J, Broglia L, Brunengo A, Burkhardt H, Chauvie S, Chuma J, Chytracek R, Cooperman G, Cosmo G, Degtyarenko P, Dell'Acqua A, Depaola G, Dietrich D, Enami R, Feliciello A, Ferguson C, Fesefeldt H, Folger G, Foppiano F, Forti A, Garelli S, Giani S, Giannitrapani R, Gibin D, Gomez Cadenas JJ, Gonzalez I, Gracia Abril G, Greeniaus G, Greiner W, Grichine V, Grossheim A, Guatelli S, Gumplinger P, Hamatsu R, Hashimoto K, Hasui

H, Heikkinen A, Howard A, Ivanchenko V, Johnson A, Jones FW, Kallenbach J, Kanaya N, Kawabata M, Kawabata Y, Kawaguti M, Kelner S, Kent P, Kimura A, Kodama T, Kokoulin R, Kossov M, Kurashige H, Lamanna E, Lampen T, Lara V, Lefebure V, Lei F, Liendl M, Lockman W, Longo F, Magni S, Maire M, Medernach E, Minamimoto K, Mora de Freitas P, Morita Y, Murakami K, Nagamatu M, Nartallo R, Nieminen P, Nishimura T, Ohtsubo K, Okamura M, O'Neale S, Oohata Y, Paech K, Perl J, Pfeiffer A, Pia MG, Ranjard F, Rybin A, Sadilov S, Di Salvo E, Santin G, Sasaki T, Savvas N, Sawada Y, Scherer S, Sei S, Sirotenko V, Smith D, Starkov N, Stoecker H, Sulkimo J, Takahata M, Tanaka S, Tcherniaev E, Safai Tehrani E, Tropeano M, Truscott P, Uno H, Urban L, Urban P, Verderi M, Walkden A, Wander W, Weber H, Wellisch JP, Wenaus T, Williams DC, Wright D, Yamada T, Yoshida H, Zschiesche D. GEANT4 - a simulation toolkit. Nuclear Instruments and Methods in Physics Research. 2003; A 506:250–303.

Ahlen SP. Theoretical and experimental aspects of the energy loss of relativistic heavily ionizing particles. Reviews of Modern Physics. 1980; 52:121–173.

Andreo P. On the clinical spatial resolution achievable with protons and heavier charged particle radiotherapy beams. Phys Med Biol. 2009; 54:N205–N215. [PubMed: 19436099]

Andreo P, Medin J, Bielajew AF. Constraints of the multiple-scattering theory of Moliere in Monte Carlo simulations of the transport of charged particles. Medical Physics. 1993; 20:1315–1325. [PubMed: 8289712]

Bednarz B, Daartz J, Paganetti H. Dosimetric accuracy of planning and delivering small proton therapy fields. Phys Med Biol. 2010; 55:7425–7438. [PubMed: 21098920]

Bednarz B, Lu HM, Engelsman M, Paganetti H. Uncertainties and correction methods when modeling passive scattering proton therapy treatment heads with Monte Carlo. Phys Med Biol. 2011; 56:2837–2854. [PubMed: 21478569]

Bichsel H, Hiraoka T. Energy loss of 70 MeV protons in elements. Nuclear Instruments and Methods in Physics Research. 1992; B66:345–351.

Chvetsov AV, Paige SL. The influence of CT image noise on proton range calculation in radiotherapy planning. Phys Med Biol. 2010; 55:N141–N149. [PubMed: 20182006]

du Plessis FCP, Willemse CA, Loetter MG, Goedhals L. The indirect use of CT numbers to establish material properties needed for Monte Carlo calculation of dose distributions in patients. Medical Physics. 1998; 25:1195–1201. [PubMed: 9682205]

Espana S, Paganetti H. The impact of uncertainties in the CT conversion algorithm when predicting proton beam ranges in patients from dose and PET-activity distributions. Physics in Medicine and Biology. 2010; 55:7557–7572. [PubMed: 21098912]

Espana S, Paganetti H. Uncertainties in planned dose due to the limited voxel size of the planning CT when treating lung tumors with proton therapy. Phys Med Biol. 2011; 56:3843–3856. [PubMed: 21628773]

Espana S, Zhu X, Daartz J, El Fakhri G, Bortfeld T, Paganetti H. The reliability of proton-nuclear interaction cross-section data to predict proton-induced PET images in proton therapy. Phys Med Biol. 2011; 56:2687–2698. [PubMed: 21464534]

EXFOR/CSISRS. Experimental Nuclear Reaction Data. International Atomic Energy Agency—Nuclear Data Section (Vienna, Austria). 2010 (http://www-nds.iaea.org/exfor/exfor.htm).

Ferrari A, Sala PR, Fasso A, Ranft J. FLUKA: a multi-particle transport code. CERN Yellow Report CERN 2005-10; INFN/TC 05/11, SLAC-R-773 (Geneva: CERN). 2005

Gensheimer MF, Yock TI, Liebsch NJ, Sharp GC, Paganetti H, Madan N, Grant PE, Bortfeld T. In vivo proton beam range verification using spine MRI changes. Int J Radiat Oncol Biol Phys. 2010; 78:268–275. [PubMed: 20472369]

Goitein M. The measurement of tissue heterodensity to guide charged particle radiotherapy. Int J Radiat Oncol Biol Phys. 1977; 3:27–33. [PubMed: 96060]

Goitein M. Calculation of the uncertainty in the dose delivered during radiation therapy. Med Phys. 1985; 12:608–612. [PubMed: 4046996]

Goitein M, Sisterson JM. The Influence of Thick Inhomogeneities on Charged Particle Beams. Radiation Research. 1978; 74:217–230. [PubMed: 96480]

Gottschalk B, Koehler AM, Schneider RJ, Sisterson JM, Wagner MS. Multiple Coulomb scattering of 160 MeV protons. Nuclear Instruments and Methods in Physics Research. 1993; B74:467–490.

Grassberger C, Paganetti H. Elevated LET components in clinical proton beams. Physics in Medicine and Biology. 2011; 56:6677–6691. [PubMed: 21965268]

Grassberger C, Trofimov A, Lomax A, Paganetti H. Variations in linear energy transfer within clinical proton therapy fields and the potential for biological treatment planning. International Journal of Radiation Oncology, Biology, Physics. 2011; 80:1559–1566.

Herault J, Iborra N, Serrano B, Chauvel P. Monte Carlo simulation of a protontherapy platform devoted to ocular melanoma. Med Phys. 2005; 32:910–919. [PubMed: 15895573]

ICRU. Bethesda, MD: International Commission on Radiation Units and Measurements; 1989. Tissue Substitutes in Radiation Dosimetry and Measurement. Report No. 44

ICRU. Bethesda, MD: International Commision on Radiation Units and Measurements; 1992. Photon, Electron, Proton and Neutron Interaction Data for Body Tissues. Report No. 46

ICRU. Bethesda, MD: International Commission on Radiation Units and Measurements; 1993. Stopping Powers and Ranges for Protons and Alpha Particles. Report No. 49

ICRU. Bethesda, MD: International Commission on Radiation Units and Measurements; 2000. Nuclear Data for Neutron and Proton Radiotherapy and for Radiation Protection. Report No. 63

Jaekel O, Reiss P. The influence of metal artefacts on the range of ion beams. Physics in Medicine and Biology. 2007; 52:635–644. [PubMed: 17228110]

Janni JF. Proton range energy tables, 1 keV - 10 GeV. Atomic Data and Nuclear Data Tables. 1982; 27:147–529.

Jiang H, Paganetti H. Adaptation of GEANT4 to Monte Carlo dose calculations based on CT data. Medical Physics. 2004; 31:2811–2818. [PubMed: 15543788]

Kimstrand P, Tilly N, Ahnesjo A, Traneus E. Experimental test of Monte Carlo proton transport at grazing incidence in GEANT4, FLUKA and MCNPX. Phys Med Biol. 2008; 53:1115–1129. [PubMed: 18263962]

Knopf A, Parodi K, Bortfeld T, Shih HA, Paganetti H. Systematic analysis of biological and physical limitations of proton beam range verification with offline PET/CT scans. Phys Med Biol. 2009; 54:4477–4495. [PubMed: 19556685]

Knopf AC, Parodi K, Paganetti H, Bortfeld T, Daartz J, Engelsman M, Liebsch N, Shih H. Accuracy of proton beam range verification using post-treatment positron emission tomography/computed tomography as function of treatment site. Int J Radiat Oncol Biol Phys. 2011; 79:297–304. [PubMed: 20646839]

Kumazaki Y, Akagi T, Yanou T, Suga D, Hishikawa Y, Teshima T. Determination of the mean excitation energy of water from proton beam ranges. Radiation Measurements. 2007; 42:1683–1691.

Litzenberg DW, Roberts DA, Lee MY, Pham K, Vander Molen AM, Ronningen R, Becchetti FD. On-line monitoring of radiotherapy beams: experimental results with proton beams. Med Phys. 1999; 26:992–1006. [PubMed: 10436901]

Lu HM. A point dose method for in vivo range verification in proton therapy. Phys Med Biol. 2008a; 53:N415–N422. [PubMed: 18997263]

Lu HM. A potential method for in vivo range verification in proton therapy treatment. Phys Med Biol. 2008b; 53:1413–1424. [PubMed: 18296770]

Matsufuji N, Tomura H, Futami Y, Yamashita H, Higashi A, Minohara S, Endo M, Kanai T. Relationship between CT number and electron density, scatter angle and nuclear reaction for hadron-therapy treatment planning. Physics in Medicine and Biology. 1998; 43:3261–3275. [PubMed: 9832015]

Moteabbed M, Espana S, Paganetti H. Monte Carlo patient study on the comparison of prompt gamma and PET imaging for range verification in proton therapy. Physics in Medicine and Biology. 2011; 56:1063–1082. [PubMed: 21263174]

Mustafa AAM, Jackson DF. The relation between x-ray CT numbers and charged particle stopping powers and its significance for radiotherapy treatment planning. Physics in Medicine and Biology. 1983; 28:169–176. [PubMed: 6408654]

Newhauser WD, Giebeler A, Langen KM, Mirkovic D, Mohan R. Can megavoltage computed tomography reduce proton range uncertainties in treatment plans for patients with large metal implants? Phys Med Biol. 2008; 53:2327–2344. [PubMed: 18421122]

Oelfke U, Lam GKY, Atkins MS. Proton dose monitoring with PET: quantitative studies in Lucite. Physics in Medicine and Biology. 1996; 41:177–196. [PubMed: 8685254]

Paganetti H. Calculation of the spatial variation of relative biological effectiveness in a therapeutic proton field for eye treatment. Physics in Medicine and Biology. 1998; 43:2147–2157. [PubMed: 9725595]

Paganetti H. Dose to water versus dose to medium in proton beam therapy. Physics in Medicine and Biology. 2009; 54:4399–4421. [PubMed: 19550004]

Paganetti H, Goitein M. Radiobiological significance of beam line dependent proton energy distributions in a spread-out Bragg peak. Medical Physics. 2000; 27:1119–1126. [PubMed: 10841418]

Paganetti H, Jiang H, Lee S-Y, Kooy H. Accurate Monte Carlo for nozzle design, commissioning, and quality assurance in proton therapy. Medical Physics. 2004; 31:2107–2118. [PubMed: 15305464]

Paganetti H, Jiang H, Parodi K, Slopsema R, Engelsman M. Clinical implementation of full Monte Carlo dose calculation in proton beam therapy. Phys Med Biol. 2008; 53:4825–4853. [PubMed: 18701772]

Paganetti H, Kooy H. Proton radiation in the management of localized cancer. Expert Rev Med Devices. 2010; 7:275–285. [PubMed: 20214431]

Paganetti H, Niemierko A, Ancukiewicz M, Gerweck LE, Loeffler JS, Goitein M, Suit HD. Relative biological effectiveness (RBE) values for proton beam therapy. International Journal of Radiation Oncology, Biology, Physics. 2002; 53:407–421.

Parodi K, Enghardt W. Potential application of PET in quality assurance of proton therapy. Phys Med Biol. 2000; 45:N151–N156. [PubMed: 11098922]

Parodi K, Paganetti H, Shih HA, Michaud S, Loeffler JS, DeLaney TF, Liebsch NJ, Munzenrider JE, Fischman AJ, Knopf A, Bortfeld T. Patient study of in vivo verification of beam delivery and range, using positron emission tomography and computed tomography imaging after proton therapy. Int J Radiat Oncol Biol Phys. 2007; 68:920–934. [PubMed: 17544003]

Parodi K, Poenisch F, Enghardt W. Experimental Study on the Feasibility of In-Beam PET for Accurater Monitoring of Proton Therapy. IEEE Transactions in Nuclear Science. 2005; 1

Pelowitz DBE. MCNPX User's Manual, Version 2.5.0. Los Alamos National Laboratory. 2005 LA-CP-05-0369.

Perl J, Schuemann J, Shin J, Faddegon B, Paganetti H. Topas - Fast and easy to use Monte Carlo platform for proton therapy applications. Medical Physics. 2011; 38:3754.

Petti PL. Differential-pencil-beam dose calculations for charged particles. Medical Physics. 1992; 19:137–149. [PubMed: 1320182]

Petti PL. Evaluation of a pencil-beam dose calculation technique for charged particle radiotherapy. International Journal of Radiation Oncology, Biology, Physics. 1996; 35:1049–1057.

Pflugfelder D, Wilkens JJ, Szymanowski H, Oelfke U. Quantifying lateral tissue heterogeneities in hadron therapy. Med Phys. 2007; 34:1506–1513. [PubMed: 17500481]

Pia MG, Begalli M, Lechner A, Quintieri L, Saracco P. Physics-related epistemic uncertainties in proton depth dose simulation. IEEE Transactions on Nuclear Science. 2010; 57

Polf JC, Peterson S, Ciangaru G, Gillin M, Beddar S. Prompt gamma-ray emission from biological tissues during proton irradiation: a preliminary study. Phys Med Biol. 2009a; 54:731–743. [PubMed: 19131673]

Polf JC, Peterson S, McCleskey M, Roeder BT, Spiridon A, Beddar S, Trache L. Measurement and calculation of characteristic prompt gamma ray spectra emitted during proton irradiation. Phys Med Biol. 2009b; 54:N519–N527. [PubMed: 19864704]

Robertson JB, Williams JR, Schmidt RA, Little JB, Flynn DF, Suit HD. Radiobiological Studies of a High-Energy Modulated Proton Beam Utilizing Cultured Mammalian Cells. Cancer. 1975; 35:1664–1677. [PubMed: 807318]

Sawakuchi GO, Titt U, Mirkovic D, Mohan R. Density heterogeneities and the influence of multiple Coulomb and nuclear scatterings on the Bragg peak distal edge of proton therapy beams. Phys Med Biol. 2008; 53:4605–4619. [PubMed: 18678928]

Schaffner B, Pedroni E. The precision of proton range calculations in proton radiotherapy treatment planning: experimental verification of the relation between CT-HU and proton stopping power. Physics in Medicine and Biology. 1998; 43:1579–1592. [PubMed: 9651027]

Schaffner B, Pedroni E, Lomax A. Dose calculation models for proton treatment planning using a dynamic beam delivery system: an attempt to include density heterogeeity effects in the analytical dose calculation. Physics in Medicine and Biology. 1999; 44:27–41. [PubMed: 10071873]

Schneider U, Pedroni E, Lomax A. The calibration of CT Hounsfield units for radiotherapy treatment planing. Physics in Medicine and Biology. 1996; 41:111–124. [PubMed: 8685250]

Schneider W, Bortfeld T, Schlegel W. Correlation between CT numbers and tissue parameters needed for Monte Carlo simulations of clinical dose distributions. Physics in Medicine and Biology. 2000; 45:459–478. [PubMed: 10701515]

Soukup M, Alber M. Influence of dose engine accuracy on the optimum dose distribution in intensity-modulated proton therapy treatment plans. Physics in Medicine and Biology. 2007; 52:725–740. [PubMed: 17228117]

Soukup M, Fippel M, Alber M. A pencil beam algorithm for intensity modulated proton therapy derived from Monte Carlo simulations. Physics in Medicine and Biology. 2005; 50:5089–5104. [PubMed: 16237243]

Stankovskiy A, Kerhoas-Cavata S, Ferrand R, Nauraye C, Demarzi L. Monte Carlo modelling of the treatment line of the Proton Therapy Center in Orsay. Phys Med Biol. 2009; 54:2377–2394. [PubMed: 19321923]

Szymanowski H, Oelfke U. Two-dimensional pencil beam scaling: an improved proton dose algorithm for heterogeneous media. Physics in Medicine and Biology. 2002; 47:3313–3330. [PubMed: 12375823]

Titt U, Sahoo N, Ding X, Zheng Y, Newhauser WD, Zhu XR, Polf JC, Gillin MT, Mohan R. Assessment of the accuracy of an MCNPX-based Monte Carlo simulation model for predicting three-dimensional absorbed dose distributions. Phys Med Biol. 2008a; 53:4455–4470. [PubMed: 18670050]

Titt U, Zheng Y, Vassiliev ON, Newhauser WD. Monte Carlo investigation of collimator scatter of protontherapy beams produced using the passive scattering method. Phys Med Biol. 2008b; 53:487–504. [PubMed: 18185001]

Tourovsky A, Lomax AJ, Schneider U, Pedroni E. Monte Carlo dose calculations for spot scanned proton therapy. Physics in Medicine and Biology. 2005; 50:971–981. [PubMed: 15798269]

Unkelbach J, Chan TC, Bortfeld T. Accounting for range uncertainties in the optimization of intensity modulated proton therapy. Phys Med Biol. 2007; 52:2755–2773. [PubMed: 17473350]

Urban L. Multiple scattering model in Geant4. CERN report. 2002 CERN-OPEN-2002-070.

Urie M, Goitein M, HolleyW R, Chen GTY. Degradation of the Bragg peak due to inhomogeneities. Physics in Medicine and Biology. 1986; 31:1–15. [PubMed: 3952143]

Urie M, Goitein M, Wagner M. Compensating for heterogeneities in proton radiation therapy. Phys Med Biol. 1984; 29:553–566. [PubMed: 6330772]

van Luijk P, van t' Veld AA, Zelle HD, Schippers JM. Collimator scatter and 2D dosimetry in small proton beams. Phys Med Biol. 2001; 46:653–670. [PubMed: 11277215]

Vanderstraeten B, Reynaert N, Paelinck L, Madani I, De Wagter C, De Gersem W, De Neve W, Thierens H. Accuracy of patient dose calculation for lung IMRT: A comparison of Monte Carlo, convolution/superposition, and pencil beam computations. Med Phys. 2006; 33:3149–3158. [PubMed: 17022207]

Wilson RR. Radiological Use of Fast Protons. Radiology. 1946; 47:487–491. [PubMed: 20274616]

Wouters BG, Lam GKY, Oelfke U, Gardey K, Durand RE, Skarsgard LD. RBE Measurement on the 70 MeV Proton Beam at TRIUMF using V79 cells and the High Precision Cell Sorter Assay. Radiation Research. 1996; 146:159–170. [PubMed: 8693066]

Yang M, Virshup G, Clayton J, Zhu XR, Mohan R, Dong L. Theoretical variance analysis of single- and dual-energy computed tomography methods for calculating proton stopping power ratios of biological tissues. Phys Med Biol. 2010; 55:1343–1362. [PubMed: 20145291]

Zacharatou Jarlskog C, Paganetti H. Physics settings for using the Geant4 toolkit in proton therapy. IEEE Transactions in Nuclear Science. 2008; 55:1018–1025.

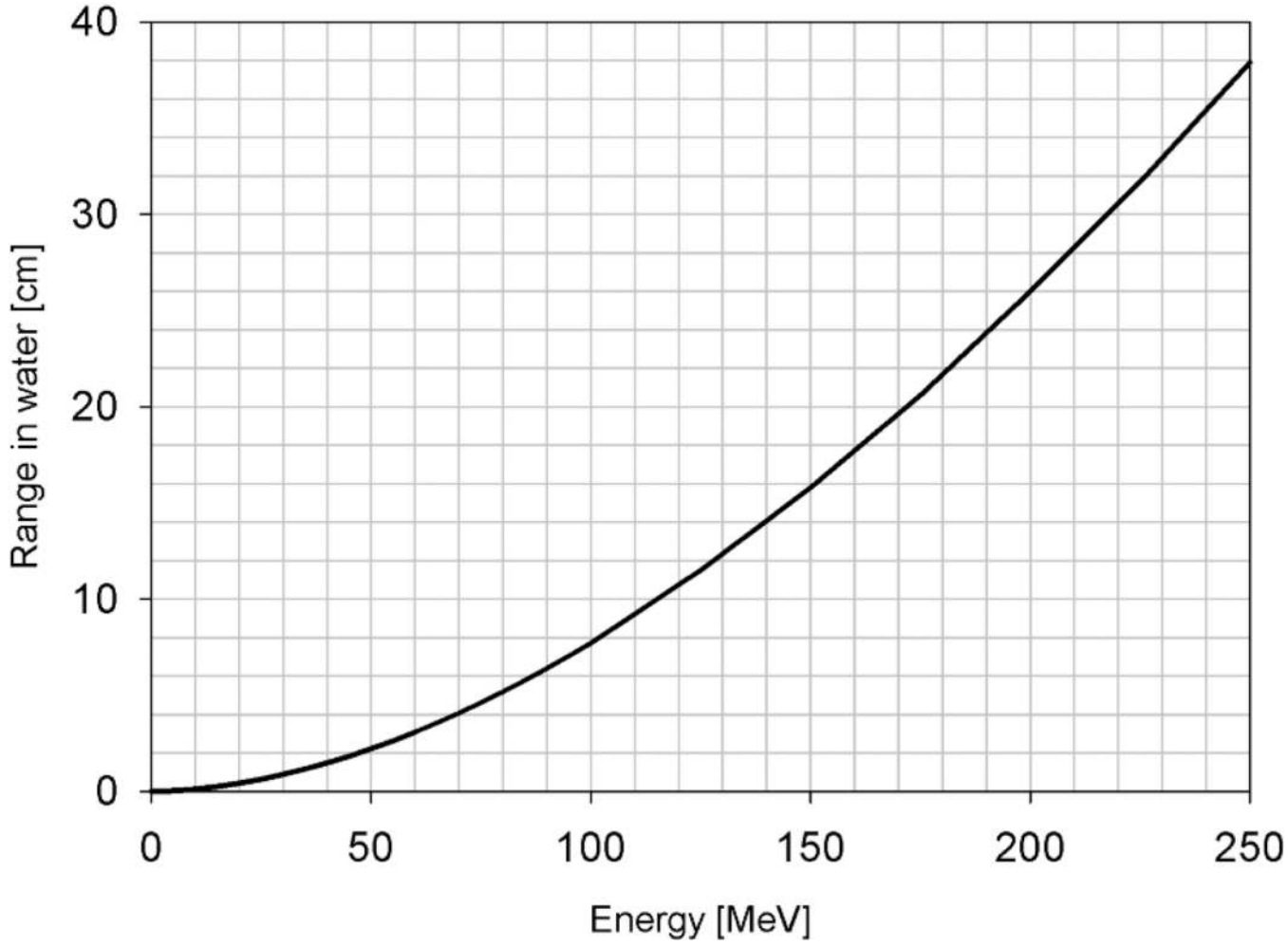

Figure 1.
Range of a proton beam in water based on the continuous slowing down approximation as a function of proton energy.

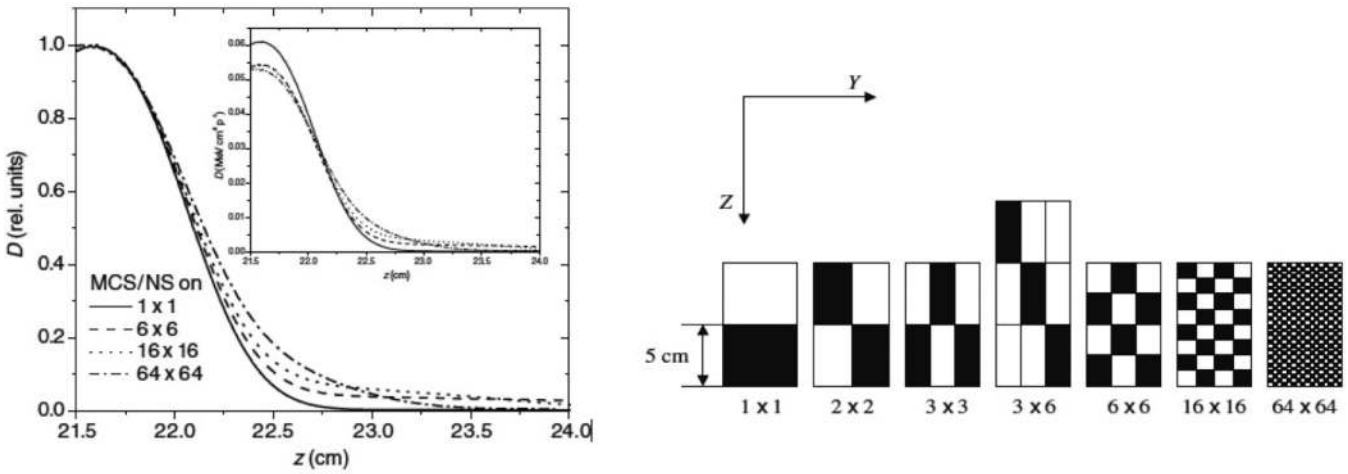

Figure 2.

Left: Distal falloff of a Bragg peak from a 220 MeV proton beam after penetrating different inhomogeneities shown on the right. The inlet shows the doses without normalization to the maximum. Adapted from (Sawakuchi *et al.*, 2008), with permission.

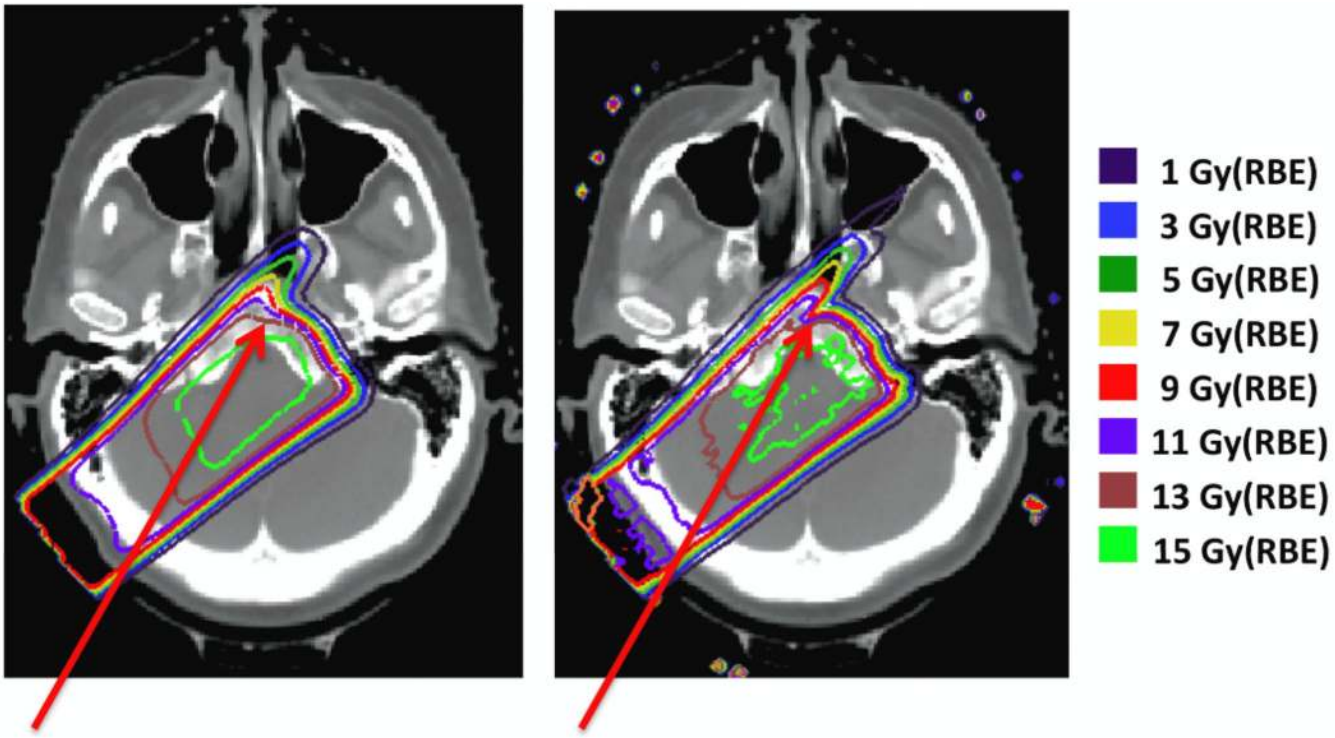

Figure 3.
Axial views of dose distributions calculated using a commercial planning system based on a pencil-beam algorithm (XiO (Computerized Medical Systems); left) and a Monte Carlo system (right). The red arrow indicates the range difference due to a density interface parallel to the beam path. Adapted from (Paganetti *et al.*, 2008), with permission.

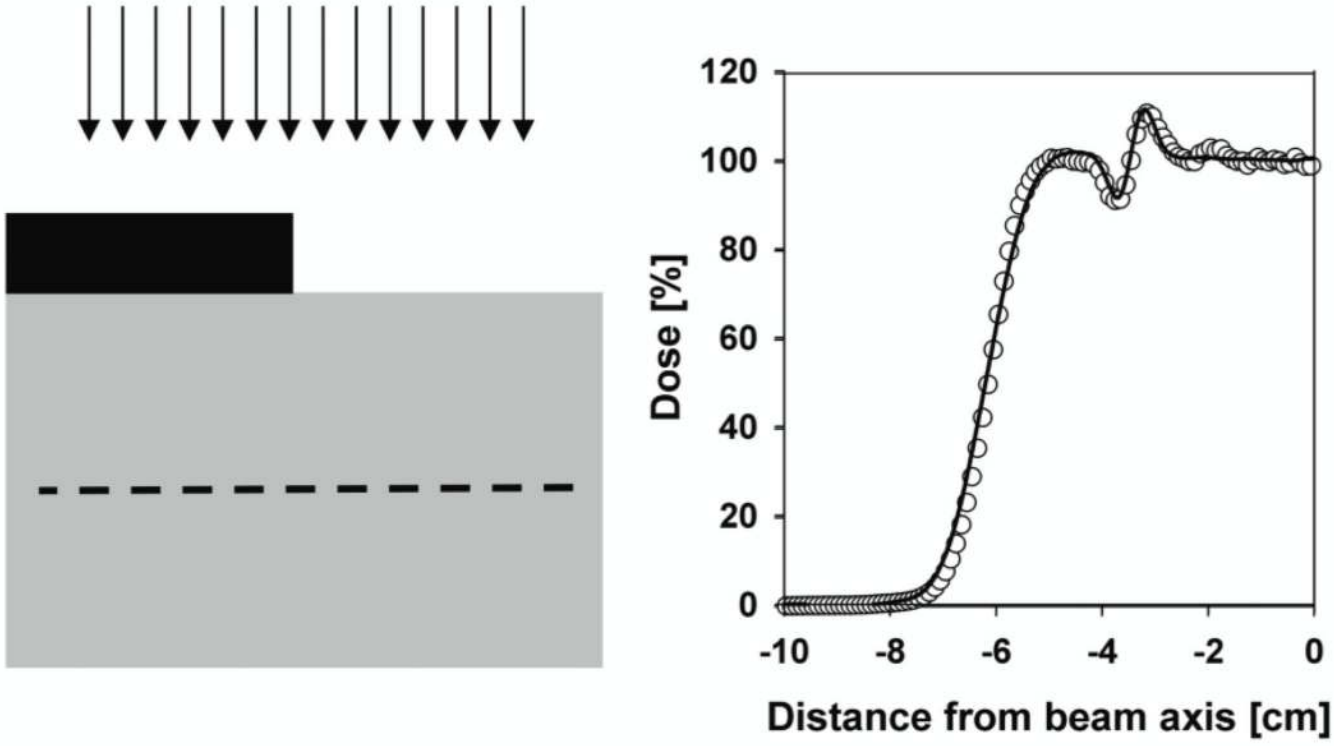

Figure 4.
Measured (circles) and Monte Carlo simulated (line) lateral dose profile. The experimental setup shown on the left consisted of a beam impinging on a half-block of bone equivalent material (black) into a water phantom (grey). The dashed line indicates the position of the measured profile. Adapted from (Paganetti *et al.*, 2008), with permission.

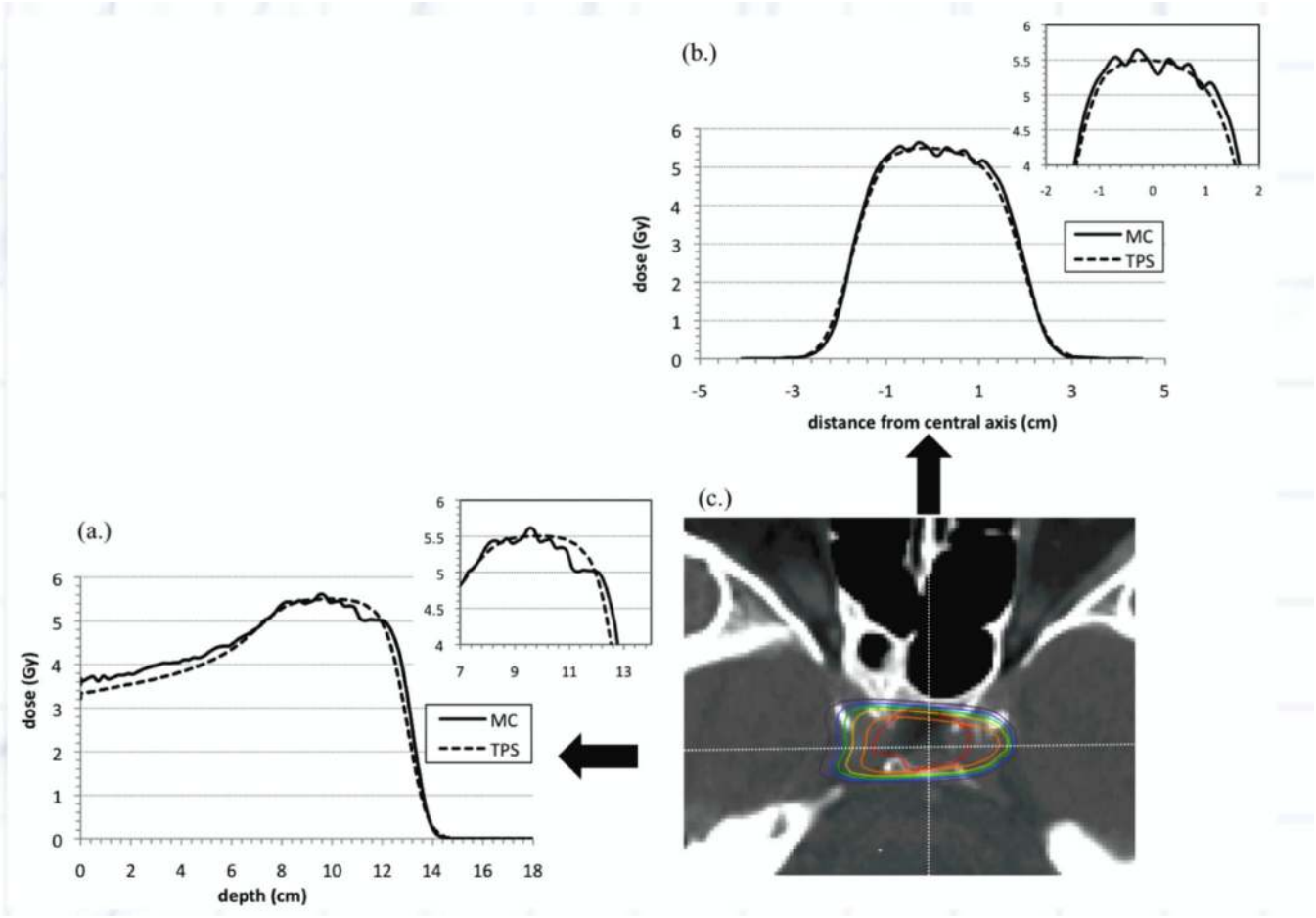

Figure 5.
Monte Carlo (MC) and analytically (TPS) generated dose distributions in a small field delivered to a head and neck patient. (a): depth dose distributions along the beam central axis; (b): transverse dose profiles; (c): axes used for figures a) and b). From (Bednarz *et al.*, 2010), with permission.

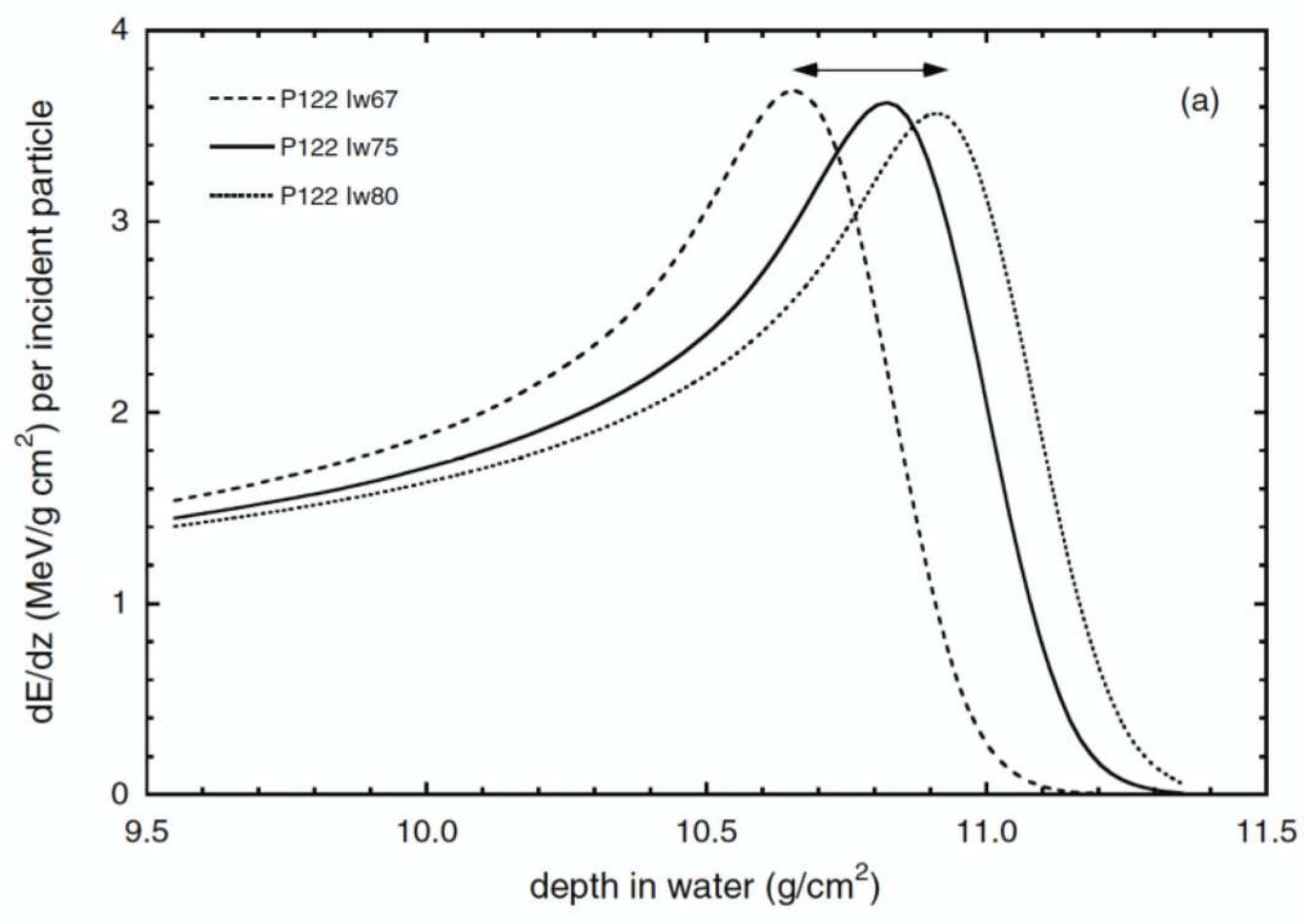

Figure 6.
Depth dose curves in water for a 122 MeV proton beam assuming mean excitation energies of 67 eV, 75 eV, and 80 eV, respectively. From (Andreo, 2009), with permission.

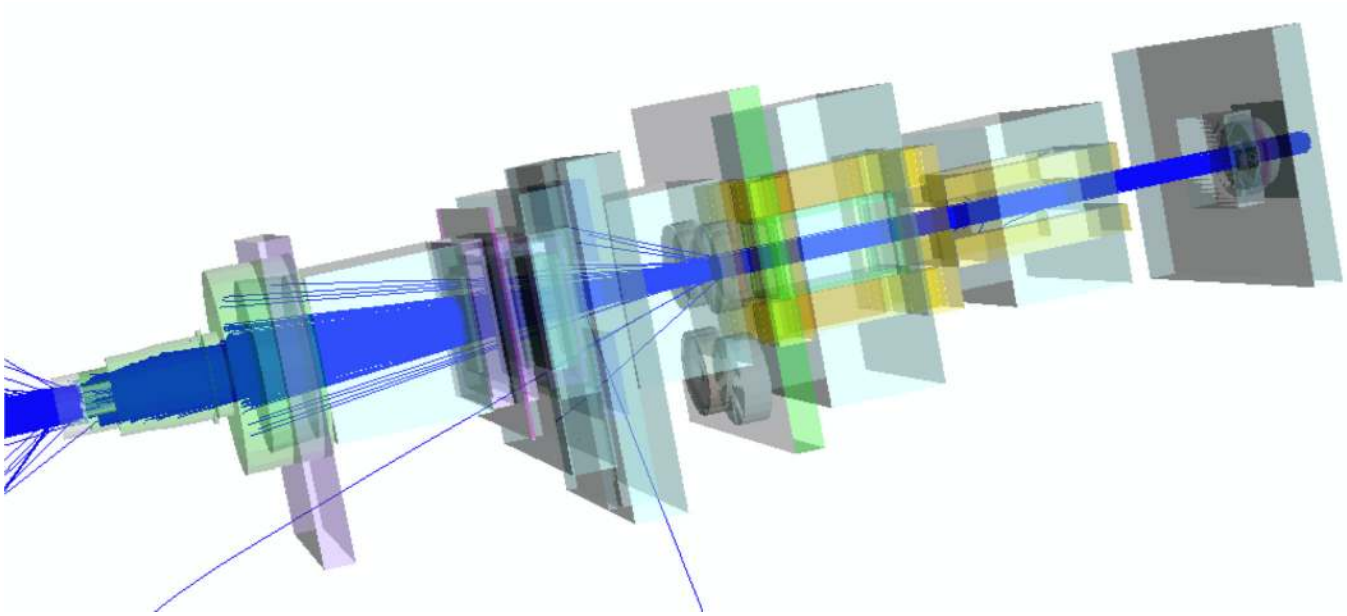

Figure 7.
Monte Carlo model of one of the treatment heads at the Francis H Burr Proton Therapy Center at Massachusetts General Hospital. The simulation was done with the TOPAS Monte Carlo system based on the Geant4 Monte Carlo code (Perl *et al.*, 2011).

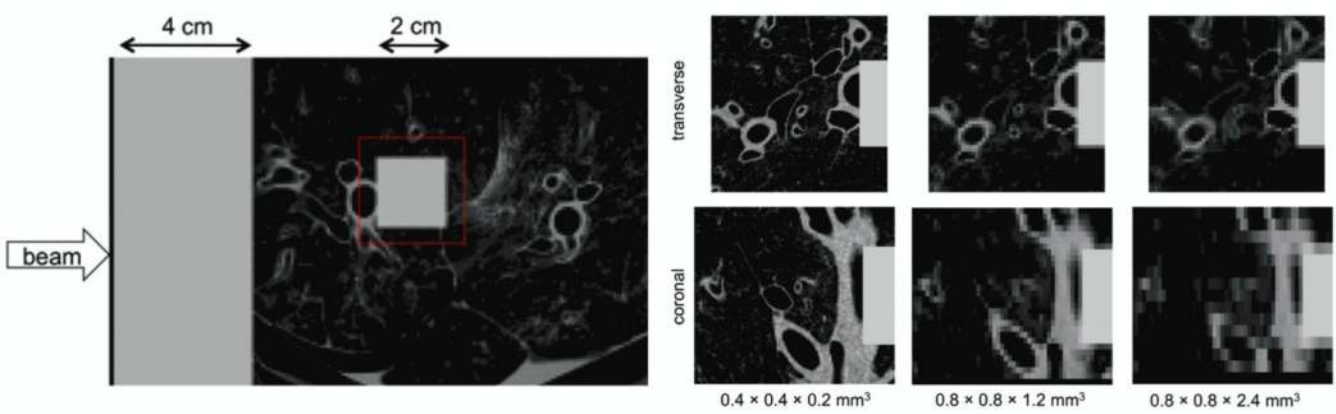

Figure 8.
Left: Image of an inflated swine lung. The CT image was edited to introduce a 4 cm thick water-equivalent entrance wall and a 2×2×2 cm^3 tumor. A 5 mm CTV expansion is shown in red. Right: Subsection of the CT image showing the transvere and coronal view of the structures for different voxel sizes. Adapted from (Espana and Paganetti, 2011), with permission.

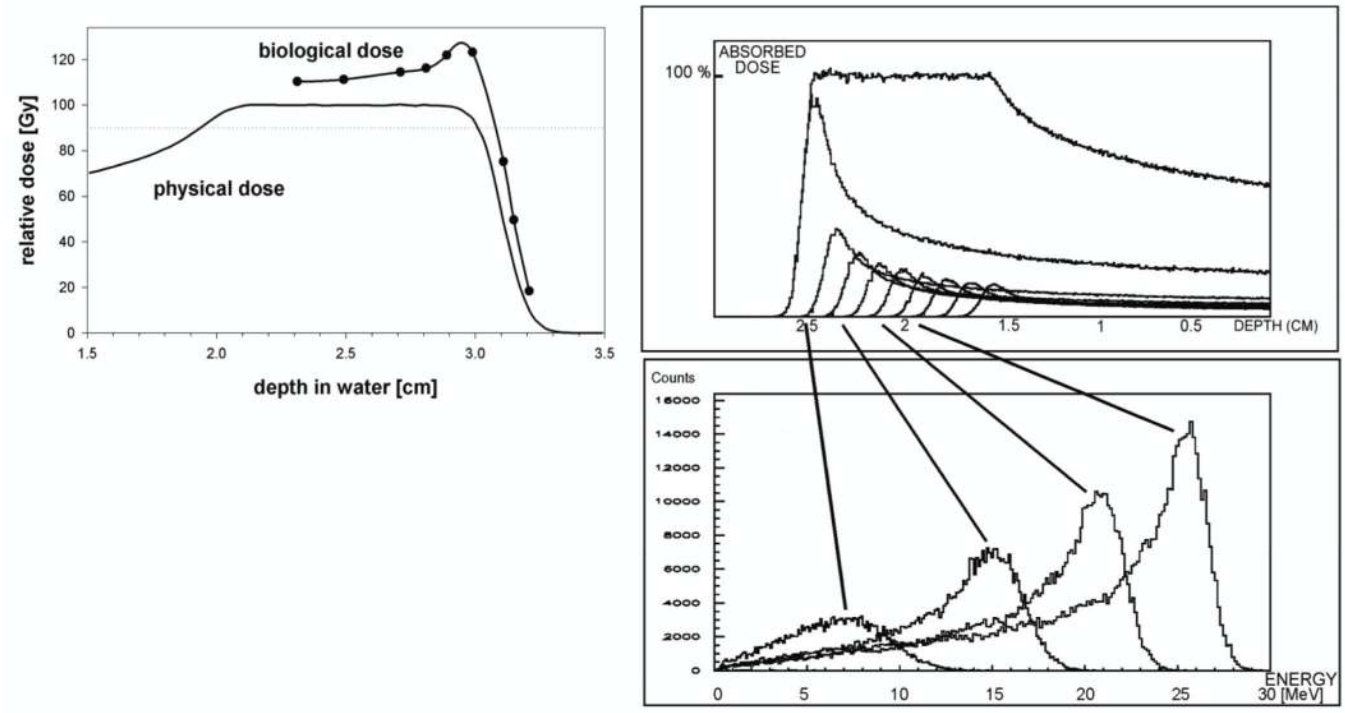

Figure 9.

Left: Physical dose and biological dose (physical dose times RBE; line with circles) simulated for one particular endpoint and dose. Right: SOBP and the underlying proton energy distributions at four different depths causing an increasing LET with depth. Adapted from (Paganetti and Goitein, 2000) and (Paganetti, 1998), with permission.

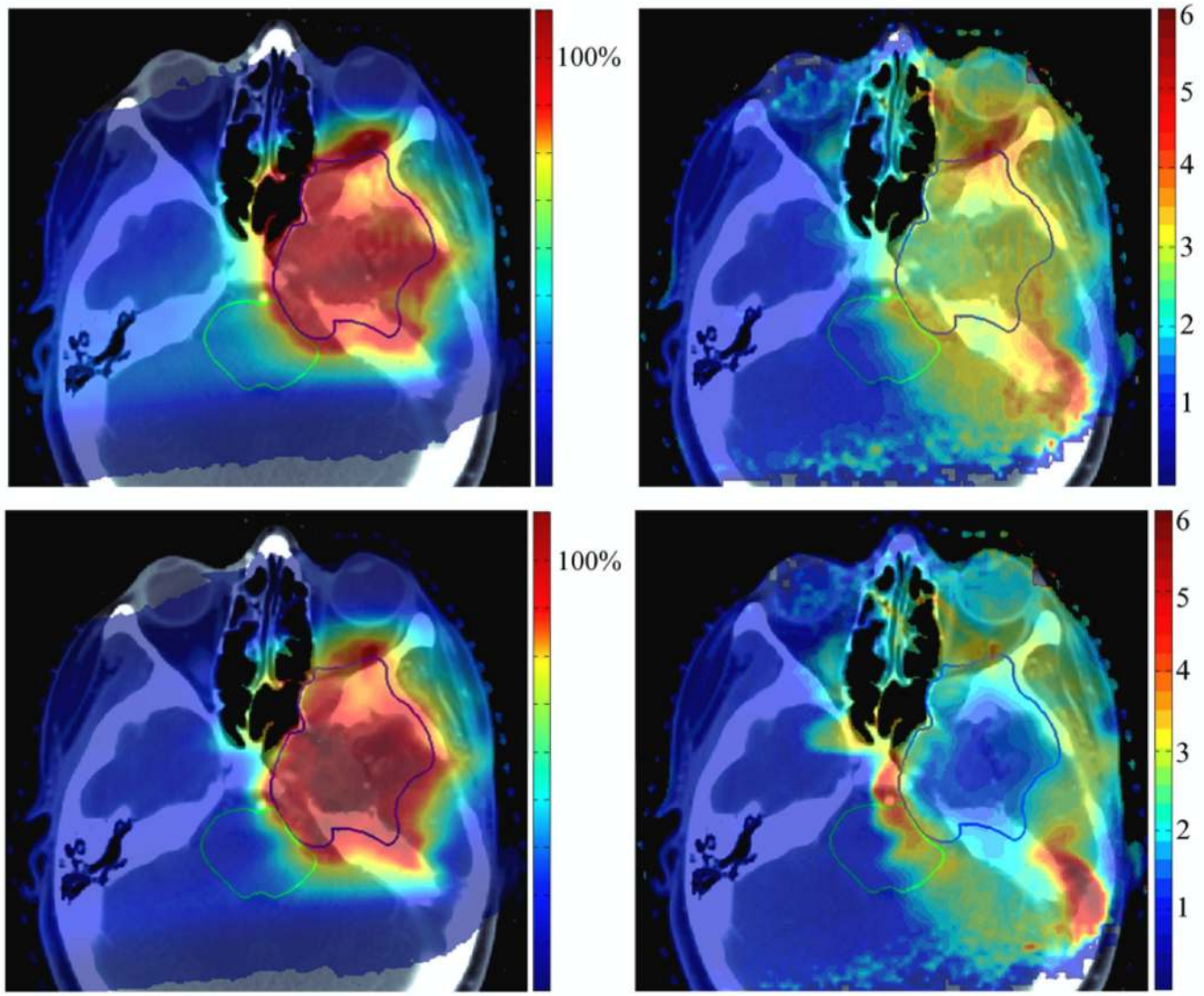

Figure 10.
Two dose distributions (left; in %) and the corresponding dose averaged LET distributions, LET_d, (right; in keV/μm) illustrating that clinically equivalent dose distributions can be achieved with quite different LET distributions steering dose falloffs away from critical structures in intensity modulated proton therapy. Based on (Grassberger *et al.*, 2011).

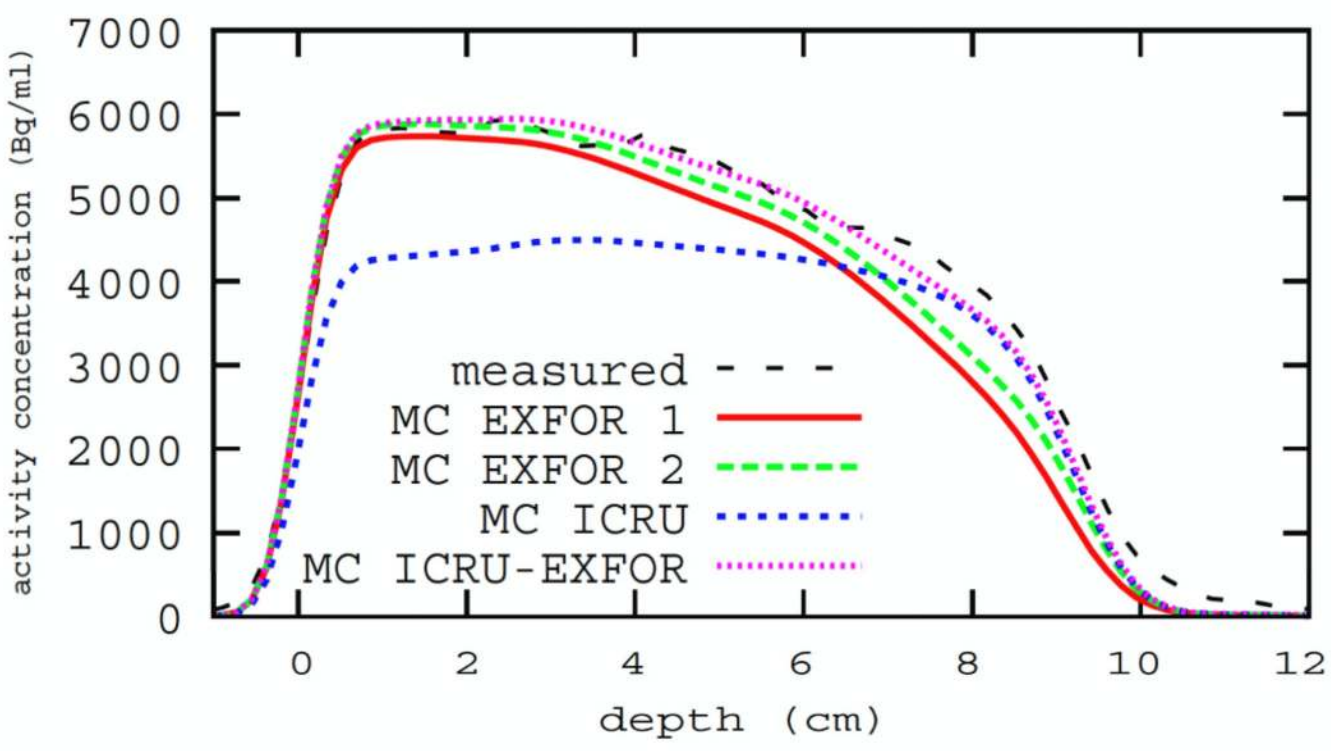

Figure 11.
Measured and Monte Carlo simulated depth activity profiles (activity concentration in Bq/ml) obtained for a gel consisting of 11.03% H, 1.04% C, 0.32% N, and 87.6% O. The scan was taken immediately after irradiation with a scan time of 5 minutes. Adapted from (Espana *et al.*, 2011), with permission.

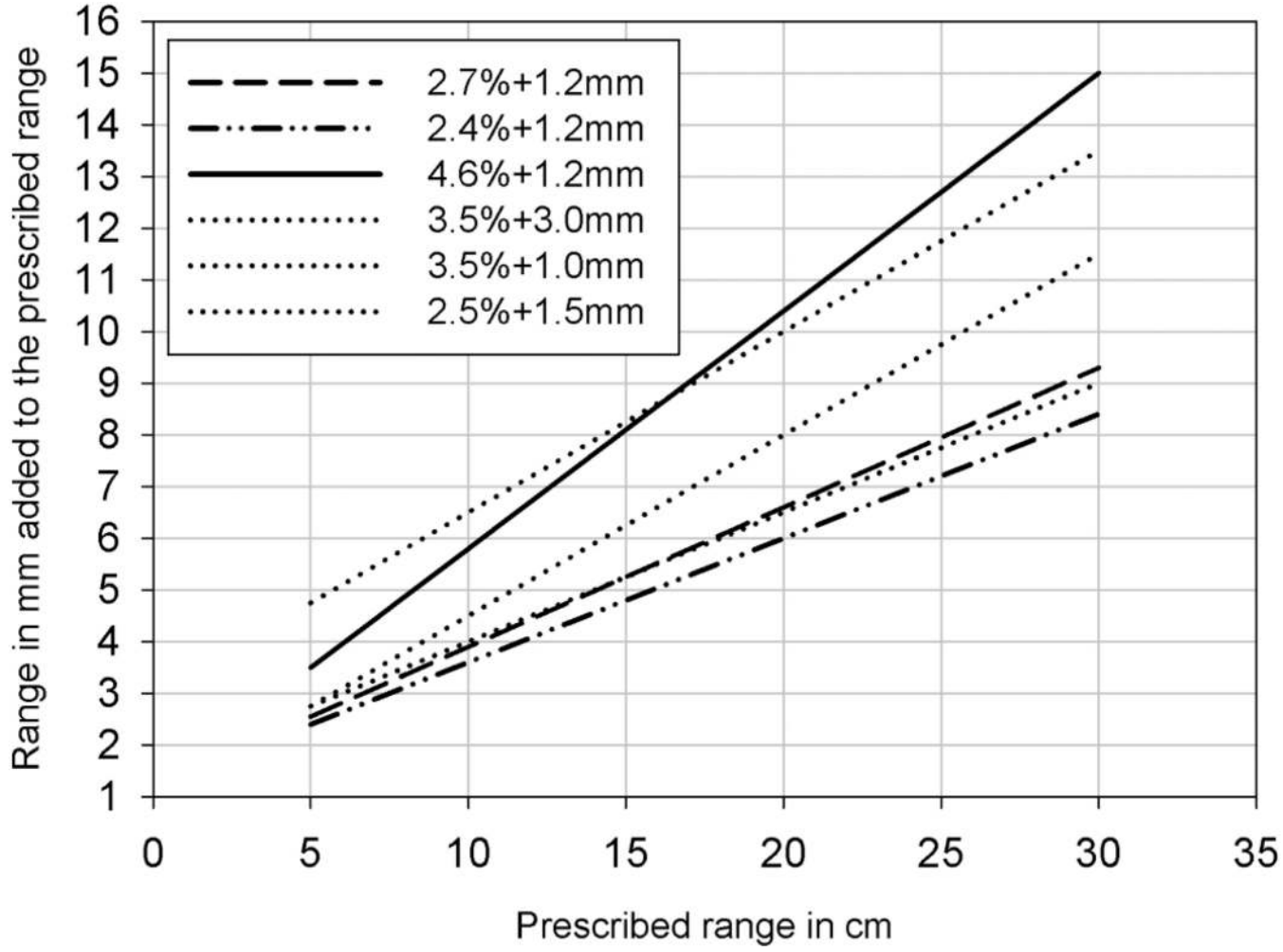

Figure 12.

Dotted lines: Typically applied range uncertainty margins in proton therapy treatment planning as currently typically applied at the Massachusetts General Hospital (3.5% + 1mm), the MD Anderson Proton Therapy Center in Houston (3.5% + 3mm), the Loma Linda University Medical Center (3.5% + 3mm), the Roberts Proton Therapy Center at the University of Pennsylvania (3.5% + 3mm), and the University of Florida Proton Therapy Institute (2.5% + 1.5mm). Note that these centers may apply bigger margins in specific treatment scenarios. Dashed line: estimated uncertainty without the use of Monte Carlo dose calculation. Solid line: estimated uncertainty for complex geometries without the use of Monte Carlo dose calculation. Dashed-dotted line: estimated uncertainty with the use of Monte Carlo dose calculation.

Table 1

Estimated proton range uncertainties and their sources and the potential of Monte Carlo for reducing the uncertainty.

Source of range uncertainty in the patient	Range uncertainty without Monte Carlo	Range uncertainty with Monte Carlo
Independent of dose calculation:		
Measurement uncertainty in water for commissioning	± 0.3 mm	± 0.3 mm
Compensator design	± 0.2 mm	± 0.2 mm
Beam reproducibility	± 0.2 mm	± 0.2 mm
Patient setup	± 0.7 mm	± 0.7 mm
Dose calculation:		
Biology (always positive) ^	+ ~0.8% [g]	+ ~0.8% [g]
CT imaging and calibration	± 0.5% [b]	± 0.5% [b]
CT conversion to tissue (excluding I-values)	± 0.5% [a]	± 0.2% [d]
CT grid size	± 0.3%	± 0.3%
Mean excitation energy (I-values) in tissues	± 1.5% [c]	± 1.5% [c]
Range degradation; complex inhomogeneities	– 0.7% [e]	± 0.1 %
Range degradation; local lateral inhomogeneities *	± 2.5% [f]	± 0.1 %
Total (excluding *, ^)	2.7% + 1.2 mm	2.4% + 1.2 mm
Total (excluding ^)	4.6% + 1.2 mm	2.4% + 1.2 mm

The number are estimations based on finding by [a](Schaffner and Pedroni, 1998; Matsufuji *et al.*, 1998);

[b](Chvetsov and Paige, 2010);

[c](ICRU, 1993; Bichsel and Hiraoka, 1992; Kumazaki *et al.*, 2007);

[d](Espana and Paganetti, 2010);

[e](Sawakuchi *et al.*, 2008; Bednarz *et al.*, 2010; Urie *et al.*, 1986);

[f](Bednarz *et al.*, 2010);

[g](Paganetti and Goitein, 2000; Robertson *et al.*, 1975; Wouters *et al.*, 1996).

The estimations are average numbers based on 1.5 standard deviations. Extreme cases, like lung, might show bigger uncertainties.